Inorg. Chem. **2007**, *46*, 3576–3584

Protein Binding to Lanthanide(III) Complexes Can Reduce the Water Exchange Rate at the Lanthanide

Stephan G. Zech,[†] Harriet B. Eldredge,[†] Mark P. Lowe,[‡] and Peter Caravan*[,†,§]

EPIX Pharmaceuticals, 67 Rogers Street, Cambridge, Massachusetts 02142, and Department of Chemistry, University of Leicester, Leicester LE1 7RH, U.K.

Received January 3, 2007

The Gd^{III}-based magnetic resonance imaging contrast agent MS-325 targets the blood protein serum albumin, resulting in an increased efficacy (relaxivity) as a relaxation agent. MS-325 showed different relaxivities when bound to serum albumin from different species, e.g., $r_1 = 30.5\ mM^{-1}\ s^{-1}$ (rabbit) vs $46.3\ mM^{-1}\ s^{-1}$ (human) at 35 °C and 0.47 T. To investigate the mechanism for this difference, surrogate complexes were prepared where the Gd^{III} ion was replaced by other Ln^{III} ions. Fluorescence lifetime measurements of the Eu^{III} analogue indicated that the hydration number was $q = 1$ and did not change when bound to either human, rat, rabbit, pig, or dog serum albumin. The Yb^{III} analogue, **YbL1**, was prepared and characterized by ^1H NMR. Line-shape analysis of the paramagnetic-shifted ^1H NMR resonances in the presence of increasing amounts of human (HSA) or rabbit (RSA) serum albumin allowed estimation of the transverse relaxation rate, R_2, of these resonances for the protein-bound **YbL1**. The rotational correlation time of **YbL1** was calculated from R_2, and the Yb–H distance and was $\tau_R = 8 \pm 1$ ns when bound to HSA and 13 ± 2 ns when bound to RSA. The water exchange rate at the Dy^{III} analogue, **DyL1**, was determined from variable-temperature R_2 measurements at 9.4 T when **DyL1** was bound to either HSA or RSA. At 37 °C, water exchange at **DyL1** was $(31 \pm 5) \times 10^6\ s^{-1}$ when bound to HSA but $(3.8 \pm 0.2) \times 10^6\ s^{-1}$ when bound to RSA. Slower water exchange upon RSA binding explains the differences in relaxivity observed. The approach of using surrogate lanthanides to identify specific molecular parameters influencing relaxivity is applicable to other protein-targeted Gd^{III} contrast agents.

Introduction

The aqueous coordination chemistry of Ln^{III} complexes has been actively studied over the last 20 years, driven largely by the medical applications of these ions. Complexes containing β-emitting isotopes of lutetium,[1] samarium,[2] promethium,[3] or holmium[4] have been used to target and destroy cancers.[5−7] Texaphyrin complexes have shown potential in photodynamic therapy (Lu) for vascular disease[8,9] and cancer[10] and also as radiosensitizers (Gd) for cancer.[11,12] The unique optical properties of lanthanides, notably terbium and europium, have resulted in many biophysical applications

* To whom correspondence should be addressed. E-mail: caravan@nmr.mgh.harvard.edu. Fax: 617-726-7422.
† EPIX Pharmaceuticals.
‡ University of Leicester.
§ Current address: Athinoula A. Martinos Center for Biomedical Imaging, Department of Radiology, Massachusetts General Hospital, Charlestown, MA 02129.

(1) Johnson, C. V.; Shelton, T.; Smith, C. J.; Ma, L.; Perry, M. C.; Volkert, W. A.; Hoffman, T. J. *Cancer Biother. Radiopharm.* **2006**, *21*, 155−166.
(2) Serafini, A. N. *Q. J. Nucl. Med.* **2001**, *45*, 91−99.
(3) Hu, F.; Cutler, C. S.; Hoffman, T.; Sieckman, G.; Volkert, W. A.; Jurisson, S. S. *Nucl. Med. Biol.* **2002**, *29*, 423−430.
(4) Kim, J. K.; Han, K. H.; Lee, J. T.; Paik, Y. H.; Ahn, S. H.; Lee, J. D.; Lee, K. S.; Chon, C. Y.; Moon, Y. M. *Clin. Cancer Res.* **2006**, *12*, 543−548.
(5) Krenning, E. P.; Teunissen, J. J.; Valkema, R.; deHerder, W. W.; deJong, M.; Kwekkeboom, D. J. *J. Endocrinol. Invest.* **2005**, *28*, 146−150.
(6) Liu, S. *Chem. Soc. Rev.* **2004**, *33*, 445−461.
(7) Zhang, H.; Chen, J.; Waldherr, C.; Hinni, K.; Waser, B.; Reubi, J. C.; Maecke, H. R. *Cancer Res.* **2004**, *64*, 6707−6715.
(8) Kereiakes, D. J.; Szyniszewski, A. M.; Wahr, D.; Herrmann, H. C.; Simon, D. I.; Rogers, C.; Kramer, P.; Shear, W.; Yeung, A. C.; Shunk, K. A.; Chou, T. M.; Popma, J.; Fitzgerald, P.; Carroll, T. E.; Forer, D.; Adelman, D. C. *Circulation* **2003**, *108*, 1310−1315.
(9) Chen, Z.; Woodburn, K. W.; Shi, C.; Adelman, D. C.; Rogers, C.; Simon, D. I. *Arterioscler., Thromb., Vasc. Biol.* **2001**, *21*, 759−764.
(10) Du, K. L.; Mick, R.; Busch, T. M.; Zhu, T. C.; Finlay, J. C.; Yu, G.; Yodh, A. G.; Malkowicz, S. B.; Smith, D.; Whittington, R.; Stripp, D.; Hahn, S. M. *Lasers Surg. Med.* **2006**, *38*, 427−434.
(11) Evens, A. M. *Curr. Opin. Oncol.* **2004**, *16*, 576−580.
(12) Meyers, C. A.; Smith, J. A.; Bezjak, A.; Mehta, M. P.; Liebmann, J.; Illidge, T.; Kunkler, I.; Caudrelier, J. M.; Eisenberg, P. D.; Meerwaldt, J.; Siemers, R.; Carrie, C.; Gaspar, L. E.; Curran, W.; Phan, S. C.; Miller, R. A.; Renschler, M. F. *J. Clin. Oncol.* **2004**, *22*, 157−165.

10.1021/ic070011u CCC: $37.00
Published on Web 04/11/2007

such as time-resolved fluorescence assays.[13,14] A lanthanum carbonate formulation has recently been approved for treating hyperphosphataemia in patients with kidney failure.[15,16] Gadolinium complexes are widely used in radiology as contrast agents for magnetic resonance imaging (MRI) scans.[17,18]

Gadolinium complexes act as relaxation agents, reducing the T_1 and T_2 of water protons and thereby generating contrast in T_1-weighted magnetic resonance images. The efficiency of a given complex as a relaxation agent is termed relaxivity, r_1, and corresponds to the change in the relaxation rate normalized to the concentration of gadolinium ($r_1 = \Delta(1/T_1)/[\mathrm{Gd}]$). Higher relaxivity compared to those of existing agents results in greater contrast or equivalent contrast at a lower dose. Much effort has gone into making high-relaxivity complexes in order to expand the applications of contrast-enhanced MRI.[19]

Relaxivity depends on a number of factors: the applied field (B_0), the hydration number (q), electronic relaxation (T_{1e}), the correlation time for rotational motion (τ_R), the rate of water exchange at the metal ion ($k_{ex} = 1/\tau_m$), the number of waters in the second coordination sphere (q'), the residency time (τ_m'), and the distance to the Gd^{III} ion (r'_{GdH}).[20] Despite this complexity, the relative importance of these parameters is becoming understood. Different magnetic resonance techniques (NMR, EPR, ENDOR, and relaxometry) have been used to provide an understanding of these gadolinium complexes.[19] One of the key parameters is τ_R, the correlation time for rotational motion.[21,22] For small molecules like the $[Gd(DTPA)(H_2O)]^{2-}$ complex, this is the correlation time that determines the relaxivity of the complex at fields used for MRI. The tumbling complex creates a fluctuating magnetic field that induces nuclear transitions and causes relaxation. However, for $[Gd(DTPA)(H_2O)]^{2-}$, the tumbling rate is in the gigahertz range and nuclear relaxation is not as efficient as it could be for protons resonating at about 64 MHz (1.5 T, the predominant clinical imaging field strength).

MS-325 [(trisodium {(2-(*R*)-[(4,4-diphenylcyclohexyl)-phosphonooxymethyl]diethylenetriaminepentaacetato)(aquo)-gadolinium(III)}); Figure 1] was designed[23] to exploit the proton relaxation enhancement effect used in studying metalloproteins.[24] MS-325 is a Gd(DTPA) derivative that binds to the blood plasma protein serum albumin.[25−27]

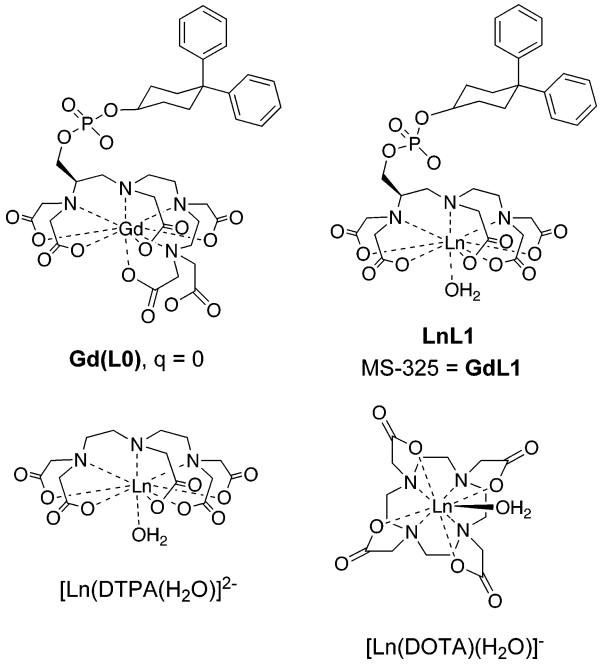

Figure 1. Lanthanide (Ln) complexes used and discussed in this study.

Binding to serum albumin restricts MS-325 to the blood vessels, resulting in its use as a blood pool imaging agent.[28,29] Reversible protein binding also results in an increased correlation time, resulting in an increased relaxivity.[26,27] For instance, in human plasma,[30] the relaxivity of MS-325 at 1.5 T is more than 6 times that of $[Gd(DTPA)(H_2O)]^{2-}$.

It was recently shown that the relaxivity of MS-325 when bound to serum albumin was dependent on the type of albumin[30] and that relaxivity did not correlate with albumin binding. For instance, the relaxivity of MS-325 bound to human (HSA) or pig serum albumin was 50% higher than that when bound to either mouse, rat, or rabbit serum albumin (RSA). It is not obvious why this should occur because there is considerable sequence homology among all of these proteins and the binding constant of MS-325 with each of these albumins was similar.[30] Clearly, when the complex is bound to the protein, there is some difference in one or more of the molecular parameters described above. If these molecular factors can be better understood, then it stands to reason that more effective relaxation agents can be designed.

(13) Bazin, H.; Trinquet, E.; Mathis, G. *J. Biotechnol.* **2002**, *82*, 233−250.
(14) Selvin, P. R. *Annu. Rev. Biophys. Biomol. Struct.* **2002**, *31*, 275−302.
(15) Fricker, S. P. *Chem. Soc. Rev.* **2006**, *35*, 524−533.
(16) Joy, M. S.; Kshirsagar, A.; Candiani, C.; Brooks, T.; Hudson, J. Q. *Ann. Pharmacother.* **2006**, *40*, 234−240.
(17) Caravan, P.; Lauffer, R. B. Contrast Agents: Basic Principles. In *Clinical Magnetic Resonance Imaging*, 3rd ed.; Edelman, R. R., Hesselink, J. R., Zlatkin, M. B., Crues, J. V., Eds.; Saunders: Philadelphia, 2005; Vol. 1, pp 357−375.
(18) Zhang, Z.; Nair, S. A.; McMurry, T. J. *Curr. Med. Chem.* **2005**, *12*, 751−778.
(19) Caravan, P. *Chem. Soc. Rev.* **2006**, *35*, 512−523.
(20) Caravan, P.; Ellison, J. J.; McMurry, T. J.; Lauffer, R. B. *Chem. Rev.* **1999**, *99*, 2293−2352.
(21) Lauffer, R. B. *Chem. Rev.* **1987**, *87*, 901−927.
(22) Lauffer, R. B. *Magn. Reson. Med.* **1991**, *22*, 339.
(23) Lauffer, R. B.; Parmelee, D. J.; Dunham, S. U.; Ouellet, H. S.; Dolan, R. P.; Witte, S.; McMurry, T. J.; Walovitch, R. C. *Radiology* **1998**, *207*, 529−538.
(24) Dwek, R. A. *Nuclear Magnetic Resonance (N.M.R.) in Biochemistry*; Oxford University Press: Oxford, U.K., 1973.
(25) Aime, S.; Chiaussa, M.; Digilio, G.; Gianolio, E.; Terreno, E. *J. Biol. Inorg. Chem.* **1999**, *4*, 766−774.
(26) Caravan, P.; Cloutier, N. J.; Greenfield, M. T.; McDermid, S. A.; Dunham, S. U.; Bulte, J. W. M.; Amedio, J. C., Jr.; Looby, R. J.; Supkowski, R. M.; Horrocks, W. D., Jr.; McMurry, T. J.; Lauffer, R. B. *J. Am. Chem. Soc.* **2002**, *124*, 3152−3162.
(27) Muller, R. N.; Radüchel, B.; Laurent, S.; Platzek, J.; Piérart, C.; Mareski, P.; Vander Elst, L. *Eur. J. Inorg. Chem.* **1999**, 1949−1955.
(28) Goyen, M.; Edelman, M.; Perreault, P.; O'Riordan, E.; Bertoni, H.; Taylor, J.; Siragusa, D.; Sharafuddin, M.; Mohler, E. R.; Breger, R.; Yucel, E. K.; Shamsi, K.; Weisskoff, R. M. *Radiology* **2005**, *236*, 825−833.
(29) Rapp, J. H.; Wolff, S. D.; Quinn, S. F.; Soto, J. A.; Meranze, S. G.; Muluk, S.; Blebea, J.; Johnson, S. P.; Rofsky, N. M.; Duerinckx, A.; Foster, G. S.; Kent, K. C.; Moneta, G.; Middlebrook, M. R.; Narra, V. R.; Toombs, B. D.; Pollak, J.; Yucel, E. K.; Shamsi, K.; Weisskoff, R. M. *Radiology* **2005**, *236*, 71−78.
(30) Eldredge, H. B.; Spiller, M.; Chasse, J. M.; Greenfield, M. T.; Caravan, P. *Invest. Radiol.* **2006**, *41*, 229−243.

Unfortunately, some of the methods used to characterize gadolinium complexes are not applicable to protein solutions for sensitivity reasons; the protein limits the concentrations of the complex that can be achieved under conditions where the protein is in excess and the metal complex is completely protein bound. In this paper, a surrogate ion approach is taken to better characterize the protein−metal complex interaction. The unique magnetic/optical properties of the lanthanides are exploited to explore specific molecular factors such as hydration, water exchange, and rotational diffusion. These methods are effective at the concentrations required for protein−complex interactions and can be generalized to other protein-targeted contrast agents.

The chemistry of Ln^{III} ions is very similar: complexes are often isostructural, and metal−ligand stability constants are similar, as are reaction kinetics.[31,32] This boring similarity in chemistry has proved useful in the applications of these ions. For instance, the ligands used to give stable gadolinium complexes developed for MRI applications are also employed to give stable Lu-177 complexes for radiotherapy.[33] Changing the ion is also done for mechanistic reasons. For instance, the luminescence lifetime of Eu^{III} can be used to estimate the hydration number of a given Eu^{III} complex.[34,35]

In this report, different Ln^{III} analogues of MS-325 are prepared and studied in the absence or presence of either HSA or RSA. By exploitation of the different properties of Gd^{III}, Eu^{III}, Dy^{III}, and Yb^{III}, the underlying mechanistic reason for this difference in relaxivity could be explained. This approach may prove useful in the better understanding of the relaxation behavior of other MRI contrast agents in protein solutions or other biological media.

The Yb^{III} analogue of MS-325 was prepared, and its solution NMR spectrum showed well-resolved paramagnetic-shifted resonances of the ligand protons. The spectrum could be assigned by numerically simulating the shifts, thereby revealing the orientation of the magnetic susceptibility tensor. Line broadening of ligand proton reasonances in the presence of increasing protein concentration was used to estimate the rotational correlation time of the complex bound to each protein. The fluorescence lifetime of the Eu^{III} analogue was determined when bound to the proteins to ascertain if the coordinated water was displaced upon protein binding. Variable-temperature r_2 measurements on the Dy^{III} analogue were used to show that the water exchange rate is slower when MS-325 is bound to RSA than when MS-325 is bound to HSA.

Experimental Section

Materials. Lyophilized pig serum albumin (lot no. 089H7603, fraction V), dog serum albumin (lot no. 092K7603, fraction V), rat serum albumin (lot no. 062K7622, fraction V), rabbit serum albumin (lot no. 049F9300, fraction V), and human serum albumin (lot no. 109H7615, fraction V) were purchased from Sigma-Aldrich (St. Louis, MO). The protein content was determined by amino acid analysis.[30] The [(4,4-diphenylcyclohexyl)phosphonooxymethyl]-diethylenetriaminepentaacetato ligand[36] (H_6**L1**) and its gadolinium[36] (**GdL1**, MS-325), europium,[26] and dysprosium[37] complexes were prepared as described previously. Partially deuterated **L1**-d_{10} was prepared as described.[38] The tetrasodium salt of **GdL0** (Figure 1) was prepared as previously reported.[26] The salts $EuCl_3 \cdot 6H_2O$ (99.9%) and $YbCl_3 \cdot 6H_2O$ (99.9%) were obtained from Aldrich. Ultrafiltration units (UFC3LCC25, regenerated cellulose membrane of 5000 Da nominal molecular weight cutoff) were obtained from Millipore Corp. (Bedford, MA).

YbL1 and YbL1-d_{10}. The ytterbium complexes of **L1** and its decadeuterated analogue (replacement of 10 acetate CH_2 hydrogens with deuterium) were prepared in solution and not isolated. The procedure was the same for both, and **YbL1** is described as a representative example. The concentration of the ligand **L1** was determined by photometric titration with $Gd(NO_3)_3$ as described previously.[26] To a 1.73 mL solution of H_6**L1** (77.0 mM, 135 μmol) at pH 6.5 was added 55.3 mg of $YbCl_3 \cdot 6H_2O$ (143 μmol), and the pH was adjusted to 6.5 by the addition of 1 M NaOH. The solution was stirred for 30 min, and the pH was raised to 7.5 with NaOH to precipitate the excess Yb^{3+}. The solution was filtered through a 0.2 μm filter. Colorimetric analysis with xylenol orange confirmed the absence of excess metal ion. The solution was then analyzed by high-performance liquid chromatography (HPLC) with UV and positive electrospray ionization detection using a gradient of 50 mM ammonium formate with 5% (9:1 ACN/50 mM ammonium formate) to 50% (9:1 ACN/50 mM ammonium formate) over 12 min (2.0 mL min^{-1}, Kromasil C4, 4.6 × 50 mm, 3.5 μm). **YbL1** eluted at 5.0 min (>97% of total peak area, positive ion, m/z = 909 $[M + 4H]^+$). Isotopic distribution was consistent with a Yb^{III} complex. No uncomplexed ligand could be detected.

All lanthanide concentrations were determined by inductively coupled plasma mass spectroscopy (ICP-MS) on an Agilent 7500 series system.

NMR Experiments. ^1H NMR spectra were recorded on a Bruker Avance 300 or 400 MHz spectrometer equipped with double-channel ($^1H/X$) probes. The temperature was controlled to within ±1 °C using dry air cooled by an Air Jet (FTS Systems). Assignment of **YbL1** was obtained from 1D ^1H and 2D $^1H-^1H$ COSY spectra recorded at 300 MHz (~20 mM sample concentration; 5 mm tube). The transverse relaxivity of **DyL1** was measured at 400 MHz using 2 mm sample tubes with increasing concentration of the metal complex in a HSA or RSA solution (80% D_2O and 20% H_2O in 50 mM phosphate buffer). A CPMG pulse sequence and the data-fitting routine implemented in the Bruker Topspin 1.3 software were used to determine T_2 of the bulk water. The bound water chemical shift of **DyL1** was measured at 300 MHz from the induced bulk water shift at increasing metal complex concentration

(31) Brücher, E.; Sherry, A. D. Stability and Toxicity of Contrast Agents. In *Chemistry of Contrast Agents in Medical Magnetic Resonance Imaging*; Toth, E., Merbach, A. E., Eds.; Wiley: New York, 2001; pp 45−119.

(32) Cotton, F. A.; Wilkinson, G. *Advanced Inorganic Chemistry*, 5th ed.; John Wiley: New York, 1988.

(33) Liu, S.; Edwards, D. S. *Bioconjug. Chem.* **2001**, *12*, 7−34.

(34) Beeby, A.; Clarkson, I. M.; Dickins, R. S.; Faulkner, S.; Parker, D.; Royle, L.; de Sousa, A. S.; Williams, J. A. G.; Woods, M. *J. Chem. Soc., Perkin Trans. 2* **1999**, 493−504.

(35) Horrocks, W. D., Jr.; Sudnick, D. R. *J. Am. Chem. Soc.* **1979**, *101*, 334−340.

(36) McMurry, T. J.; Parmelee, D. J.; Sajiki, H.; Scott, D. M.; Ouellet, H. S.; Walovitch, R. C.; Tyeklar, Z.; Dumas, S.; Bernard, P.; Nadler, S.; Midelfort, K.; Greenfield, M.; Troughton, J.; Lauffer, R. B. *J. Med. Chem.* **2002**, *45*, 3465−3474.

(37) Caravan, P.; Greenfield, M. T.; Bulte, J. W. *Magn. Reson. Med.* **2001**, *46*, 917−922.

(38) Zech, S.; Sun, W.-C.; Jacques, V.; Caravan, P.; Astashkin, A. V.; Raitsimring, A. M. *ChemPhysChem* **2005**, *6*, 2570−2577.

Table 1. First-Order Decay Constants for 0.3 mM **EuL1** Fluorescence in H_2O or D_2O Solutions of Serum Albumin (1 mM) from Various Species and Calculated Hydration Numbers, q

serum albumin	k_{H_2O} (ms^{-1})	k_{D_2O} (ms^{-1})	q
human	1.472	0.410	0.97
pig	1.496	0.419	0.99
dog	1.507	0.423	1.00
rat	1.492	0.401	1.01
rabbit	1.467	0.392	0.99

(0−150 mM) using trimethylsilyl propionate, an internal chemical shift standard. In the fast exchange limit, the bulk water shift increases linearly with the metal concentration, $\delta_{bulk}^{obs} = f_{bound}\delta_{bound} + f_{free}\delta_{free}$, where $f_{bound} = [\mathbf{DyL1}]q/55.5M$ is derived from the concentration and $\delta_{free} = 4.7$ ppm.

A series of 12 solutions in 2 mm sample tubes (Wilmad) were prepared that contained 4 mM **YbL** and ranged in HSA concentration from 0 to 1.35 mM in a 50 mM phosphate buffer (80% D_2O and 20% H_2O). An additional eight solutions ranging from 0.20 to 0.64 mM in RSA and 4 mM **YbL1** were prepared. Line widths were determined for the strongly shifted ^1H NMR resonances as a function of the albumin content.

The T_2 of water was determined at 310 K and 9.4 T for a series of solutions that contained either 2.0 mM HSA or RSA and 0, 0.5, 1.0, or 1.5 mM **DyL1** (eight solutions in total). The T_2 measurements were repeated over the range 270−330 K for the 1.0 mM **DyL1** samples and their respective diamagnetic albumin samples.

Ultrafiltration Measurements of Protein Binding of YbL1. After the NMR studies were completed, 400 μL of the NMR sample was added to a 5000 MW ultrafiltration unit. The samples were incubated at 37 °C for 30 min, placed in prewarmed centrifuge buckets, and centrifuged for 7 min at 3500*g* at 37 °C using a Jouan GT 4 22 centrifuge. The filtrates were analyzed for the ytterbium concentration by ICP-MS. The concentration of bound **YbL1** in the protein samples was determined by subtracting the ytterbium concentration (free **YbL1**) found in the filtrate from the **YbL1** concentration of the original serum albumin samples.

Fluorescence Measurements. EuL1 solutions were prepared with various species' serum albumin: human, pig, dog, rabbit, or rat. Each solution contained 0.3 mM **EuL1** and 1.0 mM albumin in pH 7.4 phosphate-buffered saline. An aliquot of each sample was lyophilized and reconstituted with D_2O, and this process was repeated twice to exchange hydrogen with deuterium.

Excited-state lifetime measurements were made on a Jobin Yvon Horiba Fluoromax-P (using DataMax for Windows v2.2). Lifetimes were measured by excitation (395 nm direct) of the sample with a short 40 ms pulse of light (500 pulses per point) followed by monitoring of the integrated intensity of light (615 nm) emitted during a fixed gate time of 0.1 ms, at a delay time later. Delay times were set at 0.1 ms intervals, covering four or more lifetimes. Excitation and emission slits were set to 15 and 5 nm bandpasses, respectively. The obtained decay curves were fitted to a simple monoexponential first-order decay curve using Microsoft Excel.

Results

Hydration Number. Fluorescence lifetimes of the **EuL1**/albumin samples in either a H_2O or D_2O solution are listed in Table 1. The hydration number q is calculated using the empirical equation of Beeby et al. (eq 1), and these are tabulated in Table 1.

$$q = 1.2[k_{H_2O} - k_{D_2O} - 0.25] \quad (1)$$

Table 2. Experimental (300 MHz, 310 K, Estimated Uncertainty ±0.5 ppm) and Simulated[a] Proton Chemical Shifts of the DTPA Moiety of **YbL1** (See Figure 2C for Assignments and Estimated Yb−H Distances)

proton	experimental shift (ppm)	simulated shift (ppm)	Yb−H distance (Å)
1	25.6	25.0 ± 0.7	5.26
2	25.6	31.8 ± 0.6	5.50
3	111.1	110.6 ± 2.0	3.47
4	62.8	60.2 ± 1.7	3.86
5	72.0	67.0 ± 1.1	4.48
6	52.7	55.1 ± 1.1	4.31
7	106.2	106.8 ± 1.8	3.51
8	4.7	4.5 ± 1.0	4.40
9	−14.2	−14.0 ± 1.7	3.70
10	−20.3	−20.3 ± 1.1	4.35
11	−22.3	−23.0 ± 1.6	3.75
12	−31.1	−26.9 ± 1.4	4.07
13	1.7	4.5 ± 1.3	4.31
14	3.2	4.5 ± 1.9	3.72
15	17.8	17.6 ± 1.4	4.20
16	−11.5	−12.7 ± 1.2	4.31
17	−43.7	−44.2 ± 1.6	4.00
18	−47.9	−51.1 ± 1.9	3.66
19	−27.2	−28.7 ± 1.2	4.38

[a] Evaluated with the SHIFT ANALYSIS program.[42] Principal values of the magnetic susceptibility tensor are $\chi_{xx} = -1217 \pm 47$ ppm Å^{-3}, $\chi_{yy} = -2007 \pm 50$ ppm Å^{-3}, and $\chi_{zz} = 3224 \pm 46$ ppm Å^{-3}.

Solution NMR Spectrum of YbL1 and Assignment of Shifted Protons. Figure 2A shows the ^1H NMR spectrum of **YbL1** at 310 K. The lines are well resolved and show only minor changes in the chemical shift with temperature (Supporting Information, Figure S1). In contrast, the ^1H NMR spectrum of $[Yb(DTPA)]^{2-}$ exhibits a pronounced temperature dependence due to the interconversion of two isomers.[39]

HPLC analysis (Supporting Information, Figure S2) demonstrates the presence of two isomers for **YbL1** (ca. 40:60 ratio); however, their interconversion is too slow to be observed on the NMR time scale. This is corroborated by the absence of any correlations between the two isomers in exchange spectroscopy spectra (not shown). Because the slow isomer interconversion causes no observable NMR spectral changes with temperature, the chemical shift changes with temperature are due to the predicted temperature behavior of paramagnetic-shifted protons.[43] Figure 2A further suggests that the two isomers display significantly different line widths, and hence peak heights. A likely reason for this is the different internal mobilities for the two isomers. Similar NMR behavior was observed[40] for diastereomers of a related substituted DTPA complex, $[Eu(EOB\text{-}DTPA)]^{2-}$. A comparison of the spectrum of **YbL1** with the partially deuterated **L1**-d_{10} (Figure 2B) shows that 10 narrow lines disappear and thereby provides assignment for the acetate CH_2 protons. The COSY spectrum (Supporting Information, Figure S3) enables assignment of pairs of geminal protons. However, unambiguous assignment for all shifted protons could only be obtained by numeric simulation of the paramagnetic shifts. We started with the coordinates determined from an X-ray structure of MS-325 [41] and used the simulation algorithm described by

(39) Jenkins, B. G.; Lauffer, R. B. *Inorg. Chem.* **1988**, *27*, 4730−4738.
(40) Thompson, N. C.; Parker, D.; Schmitt-Willich, H.; Suelzle, D.; Muller, G.; Riehl, J. P. *Dalton Trans.* **2004**, 1892−1895.
(41) Tyeklar, Z.; McMurry, T. J.; Caravan, P. 2006, in preparation.

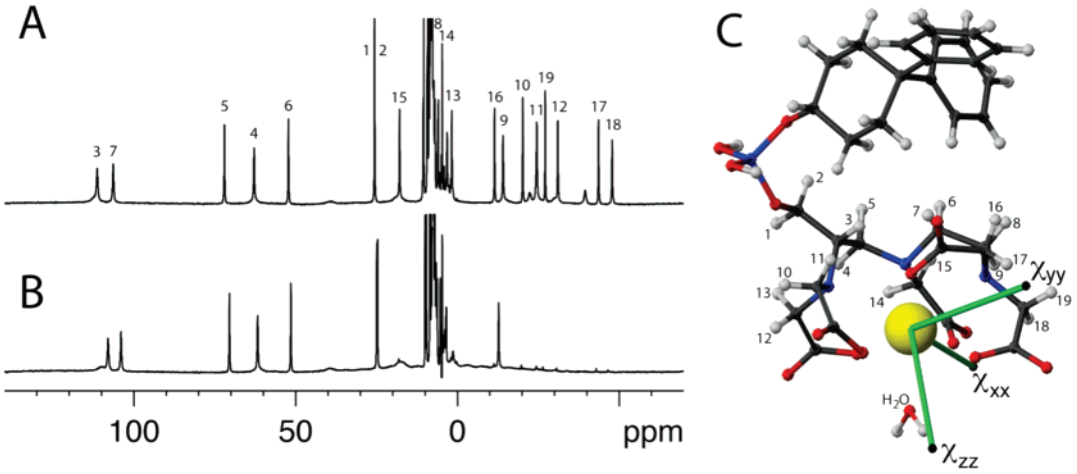

Figure 2. (A) ^{1}H NMR spectrum of **YbL1** (300 MHz, 310 K). Numbering corresponds to the assignments in part C. (B) ^{1}H NMR spectrum of decadeuterated **YbL1**-d_{10}, where acetate CH_2 protons were exchanged for deuterons. (C) **YbL1** with proton assignments for the DTPA moiety and the orientation of the principal axes of the susceptibility tensor (χ_{zz}, χ_{xx}, χ_{yy}).

Forsberg et al.[42] to arrive at a final assignment of the spectrum and the principal values and orientation of the susceptibility tensor. Table 2 summarizes the experimental and simulated shifts together with the estimated Yb−H distances at 310 K. The agreement between experimental and simulated chemical shifts is excellent, considering that in our simulations the isotropic and diamagnetic shift contributions have been neglected. The isotropic shift in **YbL1** is expected to be on the order of −3 to −5 ppm for most protons close to the metal and therefore compensates for the diamagnetic shift (ca. +2−4 ppm) as observed previously[42] for [Yb(DOTA)]$^-$.

The assignment of the protons and orientation of the magnetic susceptibility tensor as derived from simulation are depicted in Figure 2C. It is seen that the angle between the χ_{zz} axis and the M−OH_2 vector is about 26°. This is larger than that previously observed on [Ln(DOTA)]$^-$ derivatives and is a result of much lower symmetry in metal coordination with DTPA derivatives.

Estimation of the Rotational Correlation Time. At 310 K, the spectrum of **YbL1** is dominated by one isomer while the other is hardly observed (Figure 2A). This simplifies the analysis of the line broadening upon protein binding. ^{1}H NMR spectra of **YbL1** (4 mM) were recorded with increasing concentrations of either RSA or HSA (0−0.6 mM). Parts A−C of Figure 3 show the effect of the protein on the spectrum. The diamagnetic region of the **YbL1** spectrum is obscured by protein resonances, but outside this region, the paramagnetic-shifted resonances are readily seen. The line widths of these resonances were measured as a function of increasing albumin concentration. The fraction of **YbL1** not bound to albumin was then directly determined by ultrafiltration through a 5 kDa molecular weight cutoff membrane. ICP-MS was used to determine the ytterbium concentration in the initial solution and in the filtrate. The fraction bound, f^{bd}, is given by eq 2.

$$f^{bd} = 1 - \frac{[\mathbf{YbL1}]_{filtrate}}{[\mathbf{YbL1}]_{total}} \qquad (2)$$

Table 3. R_2^{bound} Values (400 MHz, 310 K) for Selected Resonances (See Figure 2C for Assignments, When **YbL1** Is Bound to HSA or RSA, and Calculated τ_R Using Eq 5 and the Yb−H Distances in Table 2)

	HSA		RSA	
proton	R_2^{bound} (s^{-1})	τ_R (ns)	R_2^{bound} (s^{-1})	τ_R (ns)
5	1545 ± 120	16.0 ± 1.1	1638 ± 150	17.0 ± 1.2
10	933 ± 50	7.7 ± 0.5	1545 ± 100	13.5 ± 1.0
12	1413 ± 60	8.0 ± 0.6	2337 ± 120	13.5 ± 1.1
15	1122 ± 60	7.8 ± 0.6	2103 ± 100	14.0 ± 1.0
17	1355 ± 80	6.6 ± 0.8	1983 ± 120	10.0 ± 1.1

The observed transverse relaxation rate, R_2^{obs}, of a given proton was estimated at its full line width at half-height, $\Delta\nu_{1/2}$ (eq 3). where LB accounts for the line broadening introduced

$$R_2^{obs} = \pi(\Delta\nu_{1/2} - LB) \qquad (3)$$

by the exponential apodization function (10 Hz) applied prior to Fourier transformation.

The binding constant of MS-325 to HSA or RSA is ca. 10^4 M^{-1}.[26,30] Hence, on the NMR time scale, the metal complex is in fast chemical exchange with the protein and this allows observation of the weighted average between the unbound complex and the protein-bound state according to

$$R_2^{obs} = f_{free}R_2^{free} + f_{bound}R_2^{bound} + R_2^{exch} \qquad (4)$$

where f represents the fraction of the complex present that is unbound (free) or bound to the protein (bound) and the observed relaxation rate has contributions from the relaxation rates of the unbound and bound complexes and those due to chemical exchange (R_2^{exch}).

Figure 3 shows a drastic increase in the line width as a function of the HSA concentration; however, the resonance frequencies are independent of the protein concentration, indicating that the paramagnetic shift is very similar for free and protein-bound **YbL1**. This renders the exchange contribution in eq 4 negligible and allows estimation of R_2^{bound}

(42) Forsberg, J. H.; Delaney, R. M.; Zhao, Q.; Harakas, G.; Chandran, R. *Inorg. Chem.* **1995**, *34*, 3705−3715.

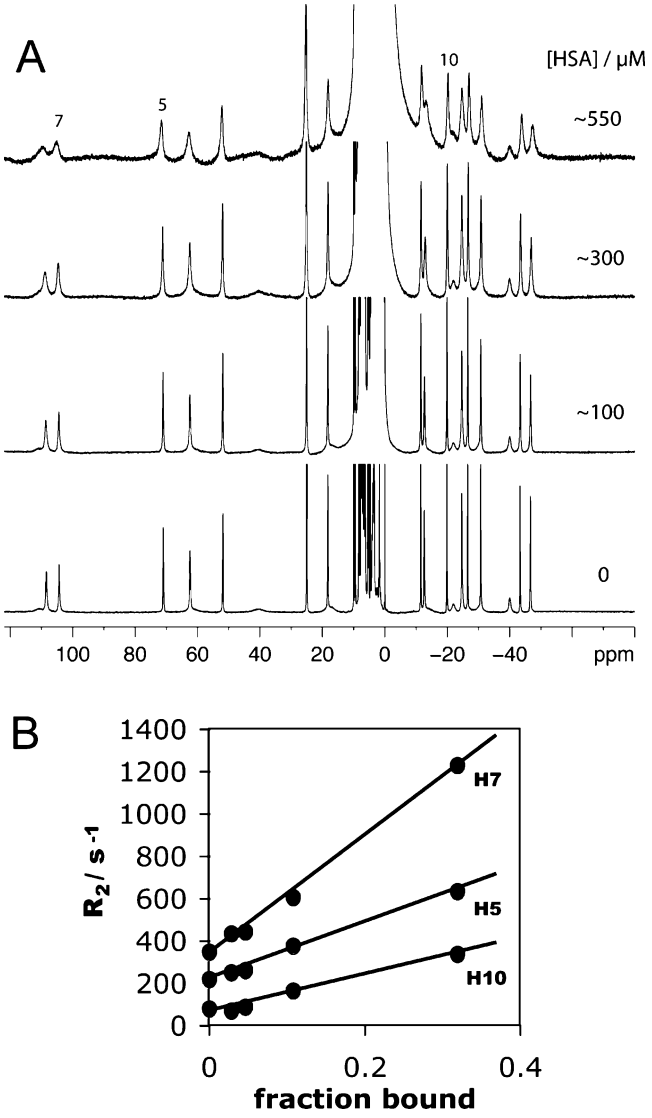

Figure 3. (A) ^{1}H NMR spectra (400 MHz, 310 K) of 4 mM **YbL1** with increasing amounts of protein HSA added. (B) Plot of the observed transverse relaxation rate of selected resonances at a given HSA concentration versus the experimentally determined fraction of **YbL1** bound to HSA under those conditions. Extrapolation to $f_{bound} = 1$ gives R_2 for the bound **YbL1** and allows calculation of the rotational correlation time.

from a plot of R_2^{obs} as a function of the fraction bound; i.e., by extrapolation to $f_{bound} \rightarrow 1$, the relaxation rate of transverse relaxation in the bound state is derived. This is illustrated in Figure 3B for selected protons in HSA solutions.

The line broadening predominantly originates from Curie spin relaxation.[43,44] Modulation of the time-averaged magnetic moment of the molecule by rotation induces nuclear relaxation in a dipolar manner. This is given by eq 5. Here

$$R_2^{Curie} = \frac{1}{5}\left(\frac{\mu_0}{4\pi}\right)^2 \frac{\omega_H^2 g_J^4 \mu_B^4 J^2 (J+1)^2}{(3kT)^2 r_{YbH}^6}\left[4\tau_c + \frac{3\tau_c}{1+\omega_H^2\tau_c^2}\right] \quad (5)$$

μ_0 is the permeability of the vacuum, ω_H is the proton Larmor frequency (rad s^{-1}), g_J is the Landé g factor for Yb^{III} ($^8/_7$), J is the vector combination of orbital and spin angular momenta ($J = {}^7/_2$ for Yb^{III}), r_{YbH} is the ion−nuclear distance, k is Boltzmann's constant, T is the absolute temperature, μ_B is the electron Bohr magneton, and τ_c is the correlation time. In this case, the correlation time corresponds to the correlation time for molecular tumbling, i.e., $\tau_c = \tau_R$. Using Yb−H distances estimated from the crystal structure of the gadolinium complex, the correlation time τ_R is readily obtained from eq 5. Table 3 lists some resonances used for line-shape analysis and their estimated correlation times in either a HSA or RSA solution.

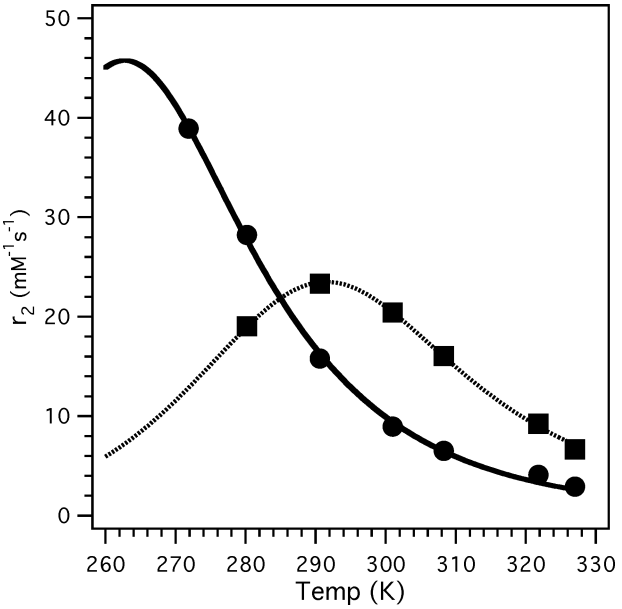

Figure 4. Transverse relaxivity (r_2) of **DyL1** in HSA (circles) or RSA (squares) at 9.4 T as a function of the temperature. The solid lines are fits to the data as described in the text.

Transverse Relaxivity, r_2, of DyL1. Relaxivities were measured at 9.4 T in the presence or absence of either RSA or HSA. The protein solutions were 2 mM, and the **DyL1** concentration ranged from 0 to 1.5 mM. The relaxivity, r_2, at 37 °C was obtained from the slope of a plot of $1/T_2$ vs [**DyL1**]. The temperature dependence on r_2 was measured from 7 to 55 °C, and the results are plotted in Figure 4.

Water Exchange at DyL1 When Bound to Albumin. Transverse relaxivity can be related to two-site exchange by eq 6, where k_{ex} is the water exchange rate, R_{2m} is the

$$r_2 = k_{ex}\left(\frac{q}{[H_2O]}\right)\left[\frac{R_{2m}^2 + R_{2m}k_{ex} + (\Delta\omega_m)^2}{(R_{2m}+k_{ex})^2 + (\Delta\omega_m)^2}\right] \quad (6)$$

transverse relaxation rate of the bound water protons, $\Delta\omega_m$ is the chemical shift of the bound water protons. In general, there is also an outer-sphere component to r_2, but it was previously shown[37] that this is very small (0.05 mM^{-1} s^{-1}) and can be neglected here. The chemical shift of the coordinated water was measured in the absence of protein, and it is assumed that the chemical shift should not change when the complex binds to albumin (no change in the chemical shift was observed upon protein binding for protons on **YbL1)**. R_{2m} is given by eq 5, except here the correlation time can also be contributed to from the water

(43) Bertini, I.; Luchinat, C. *Coord. Chem. Rev.* **1996**, *150*, 77−110.
(44) Gueron, M. *J. Magn. Reson.* **1975**, *19*, 58−66.

Table 4. Water Exchange Parameters for **DyL1** Bound to Either HSA or RSA[a]

	DyL1 + HSA	**DyL1** + RSA
k_{ex}^{310} ($\times 10^{-6}$ s^{-1})	31 ± 5	3.8 ± 0.2
$\Delta H^{\ddagger}$ (kJ mol^{-1})	22 ± 7	26 ± 1
τ_R^{310} (ns)	8	13
ΔE_R (kJ mol^{-1})	44 ± 2	80 ± 7

[a] The estimated uncertainty is 1 standard deviation and the rotational correlation time at 310 K is fixed to the value determined for the Yb^{III} analogue.

residency time, τ_m. For dipolar Curie spin relaxation with exchange, $1/\tau_c = 1/\tau_m + 1/\tau_R$. Scalar relaxation is negligible because of the weak isotropic hyperfine interaction between the Dy^{III} ion and the water proton ($A/h < 0.1$ MHz).[45,46] Solomon-type dipolar relaxation is also negligible at 9.4 T.[37]

Taking the rotational correlation times determined for the Yb^{III} complex and a chemical shift of the bound water of −650 ppm, one can compute water exchange rates of 31×10^6 s^{-1} for **DyL1** bound to HSA and 3.8×10^6 s^{-1} for **DyL1** bound to RSA at 310 K. The variable-temperature r_2 data were then analyzed. It was assumed that the temperature dependences of water exchange and rotational motion could each be described by a monoexponential function (eqs 7 and 8), where k_{ex}^{310} and τ_R^{310} are the water exchange rate and

$$k_{ex} = \frac{1}{\tau_m} = \frac{k_{ex}^{310} T}{310.15} \exp\left[\frac{\Delta H^{-}}{R}\left(\frac{1}{310.15} - \frac{1}{T}\right)\right] \quad (7)$$

$$\tau_R = \tau_R^{310} \exp\left[\frac{\Delta E_R}{R}\left(\frac{1}{T} - \frac{1}{310.15}\right)\right] \quad (8)$$

rotational correlation time at 310 K. Equation 7 is another form of the Eyring equation. The variable-temperature relaxivity data were fit using eqs 5−8, while keeping τ_R^{310} fixed to the values determined for **YbL1** in HSA and RSA. The chemical shift was assumed to vary linearly and inversely with temperature. The solid lines in Figure 4 represent the best fit to the data. The fitted parameters are given in Table 4.

Discussion

Gadolinium complexes have been widely studied recently because of their potential use as MRI contrast agents. Much effort has gone into the better understanding of the relaxation enhancement of solvent protons by different gadolinium complexes in order to produce more potent contrast agents. There are many molecular contributors to relaxation: the number of inner-sphere water molecules, the rate of water exchange from the inner sphere to the bulk, the electronic relaxation rates, molecular tumbling, and relaxation of water in the second and outer spheres. All of these can have significant effects on the overall bulk water relaxation rate.

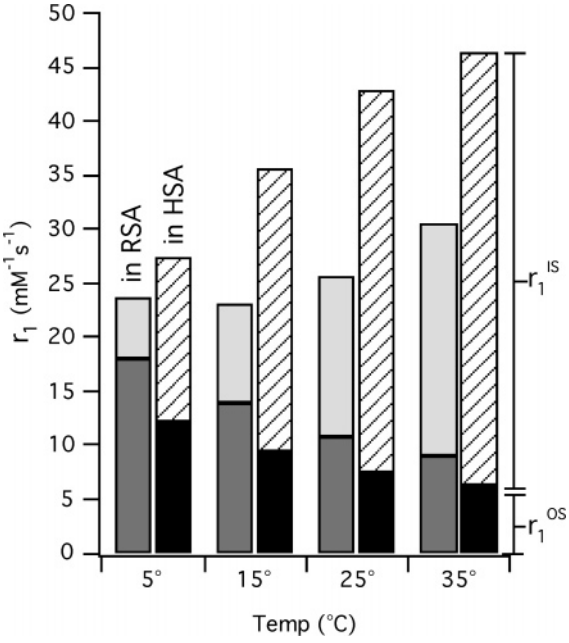

Figure 5. Longitudinal relaxivity (r_1) of MS-325 (**GdL1**) bound to RSA (light gray) or HSA (white) as a function of the temperature. Relaxivity of **GdL0** in RSA (dark gray) or HSA (black) provides an estimate of the outer/second-sphere (r_1^{OS}) contribution to the observed relaxivity of MS-325 in RSA or HSA.

Targeting a gadolinium complex to a protein or other macromolecule offers several benefits: it localizes the contrast agent at the biochemical region of interest; it increases the relaxivity of the complex by increasing the rotational correlation time; binding is reversible, which allows for eventual renal clearance of the agent.[22] This is the case with MS-325, which targets serum albumin for blood vessel imaging.[23] Relaxivity is much higher in a blood plasma or albumin solution than in the absence of protein. However, relaxivity when bound to HSA was much greater than that when bound to RSA.[30] Figure 5 shows some variable-temperature relaxivity data for MS-325 bound to either HSA or RSA.

The techniques that have been used to characterize water exchange and molecular tumbling for small molecules are less applicable to protein-bound complexes. Protein solubility often limits the concentration of the protein-bound species achievable, resulting in a lack of sensitivity. The long correlation times can result in extreme line broadening, making relaxation time measurements challenging. In addition, ^{17}O relaxation becomes multiexponential outside the extreme-narrowing limit. In this study, we used surrogates for the Gd^{III} ion in order to trace the differences in the relaxivity of MS-325.

Figure 5 shows the relaxivity of MS-325 (**GdL1**) and that of **GdL0** when bound to HSA or RSA and as a function of temperature. **GdL0** is a similar complex but is based on the TTHA ligand, which is known to coordinatively saturate Gd^{III}.[47] **GdL0** was used to estimate the relaxivity effect arising from the inner-sphere water.[26] There is a significant

(45) Astashkin, A. V.; Raitsimring, A. M.; Caravan, P. *J. Phys. Chem. A* **2004**, *108*, 1900−2001.
(46) Raitsimring, A. M.; Astashkin, A. V.; Poluektov, O. G.; Caravan, P. *Appl. Magn. Reson.* **2005**, *28*, 281−295.
(47) Ruloff, R.; Gelbrich, T.; Sieler, J.; Hoyer, E.; Beyer, L. *Z. Naturforsch., B: Chem. Sci.* **1997**, *52*, 805−809.

contribution to MS-325 relaxivity from protons outside the inner sphere, especially at low temperatures. However, the low relaxivity observed for MS-325 bound to RSA is not likely a second-sphere effect. The **GdL0** relaxivity data trend the wrong way and are slightly higher in RSA. The temperature dependence suggests that water exchange is in the slow limit because the relaxivity due to the inner-sphere water increases with the temperature. Relaxivity could be lower in RSA because (1) the inner-sphere water is being displaced by a protein side chain, (2) water exchange slows down when the complex is bound to the protein, and (3) although the complex is bound to the protein, there is some fast internal motion limiting relaxivity.

There are examples of Gd^{III} complexes bound to serum albumin where the hydration number q decreases when the complex is bound to the protein,[38,48] presumably because the high local concentration of a carboxylate or hydroxyl side chain can coordinate the gadolinium and displace the waters. Two examples where this was reported involved complexes that had $q = 2$ in the absence of protein and $q = 0$ in the presence.[38,48] The hydration state of the europium analogue of MS-325 bound to HSA was previously found[26] to be unchanged at $q = 1$. Fluorescence lifetime measurements of the europium analogue **EuL1** in the presence of excess human, pig, dog, rabbit, or rat serum albumin were recorded in either H_2O or D_2O and are listed in Table 1. There is an established relationship between the hydration number and the rate of quenching in H_2O because of coupling to the O−H oscillator.[34,35] These measurements indicated that $q = 1$ and does not change, regardless of the protein to which the complex is bound.

The nuclear magnetic relaxation dispersion (NMRD, field dependence on relaxivity) reported previously[30] suggested that tumbling was slowed when MS-325 binds to both albumins as expected. However, because the NMRD is dependent on many parameters, an independent measure of the tumbling rate was sought. The Yb^{III} analogue gives a well-resolved ^1H NMR spectrum with a broad chemical shift dispersion. The paramagnetic-induced pseudocontact shifts yield structural information. The magnitude of the shift depends on the distance between Yb and the proton and the angle between the vector it forms and the z axis of the susceptibility tensor, χ_{zz}. This structure is shown in Figure 2C along with the principal axis system of the susceptibility tensor. The binding of MS-325 to serum albumin is moderate ($K_a \sim 10^4\ M^{-1}$), and this results in a rapid off rate.[26] Because of this rapid chemical exchange, there is a linear increase in the transverse relaxation rate of the protons on **YbL1** as a function of added albumin. By measuring R_2 of the paramagnetically shifted protons as a function of the albumin concentration and measuring the fraction of **YbL1** bound to protein, one can extrapolate to R_2^{bound}. This relaxation rate depends on the correlation time and the Yb−H distance. The distances are estimated from the crystal structure of MS-325, and the correlation time can be computed. ^1H NMR allows the use of low concentrations, no isotopic labeling, and simple 1D spectra to determine the correlation time. The chemical shift dispersion of the **YbL1** complex ensures that there are several resonances not obscured by the broad albumin peaks. Table 3 lists the R_2^{bound} and τ_R values for selected resonances. On average, **YbL1** bound to RSA is slightly less mobile ($\tau_R \sim 13$ ns) than when bound to HSA ($\tau_R \sim 8$ ns). Proton 5 seems to be more restricted than other ligand protons, which may be explained by its proximity to the protein binding group. This demonstrates the potential of the method to obtain *local* mobilities.

As expected, τ_R was long (~10 ns) and clearly not a source of the lower relaxivity observed for MS-325 in RSA. In fact, the measured correlation time was a little longer for the RSA-bound complex. The studies with **YbL1**, **EuL1**, and **GdL0** implied that the difference in relaxivity was probably due to a difference in the water exchange rate when the complex was bound to the different proteins. The usual way to measure water exchange at Gd^{III} complexes is by measuring R_2 of solvent $H_2{}^{17}O$ as a function of the temperature.[49] These studies typically require about a 10 mM complex in order to measure a significant paramagnetic contribution to the observed rate because the relaxation rate of quadrupolar $H_2{}^{17}O$ itself is already very fast. The limited sensitivity makes it impossible to work under conditions where the protein concentration is in excess. Moreover, concentrated (1−3 mM) albumin increases the baseline diamagnetic ^{17}O rate by as much as a factor of 4, further limiting the sensitivity of this technique.

Transverse proton relaxation by the dysprosium complex proved useful for accessing the water exchange rate. The proton relaxation rate was sensitive enough that a significant paramagnetic effect could be measured under conditions where the protein was in excess and most of the paramagnetic effect was coming from the protein-bound complex. The dominant relaxation mechanism is the dipolar form of Curie spin relaxation. Unlike its Gd^{III} analogue, it was previously shown that second/outer-sphere transverse relaxivity was negligible for **DyL1**.[37] Based on ^1H ENDOR studies on Gd^{III} complexes, the isotropic hyperfine interaction between the dysprosium ion and the coordinated water proton was assumed to be less than 0.1 MHz.[46] Thus, the scalar contribution to relaxation could be neglected.

The relaxivity of the **DyL1**/albumin solutions is dependent on the Dy−H distance, the water residency time, and the rotational correlation time. The distance was assumed to be that of the aqua ion, 3.03 Å.[50] The rotational correlation time was taken from the **YbL1** line-broadening studies. This allowed the water exchange rate to be estimated at $31 \times 10^6\ s^{-1}$ for **DyL1** bound to HSA and $3.8 \times 10^6\ s^{-1}$ for **DyL1** bound to RSA at 310 K. In the absence of protein, water exchange at **DyL1** was determined to be $63 \times 10^6\ s^{-1}$ at 310 K.[37] Water exchange at **DyL1** is slightly reduced upon

(48) Aime, S.; Gianolio, E.; Terreno, E.; Giovenzana, G. B.; Pagliarin, R.; Sisti, M.; Palmisano, G.; Botta, M.; Lowe, M. P.; Parker, D. *J. Biol. Inorg. Chem.* **2000**, *5*, 488−497.

(49) Powell, D. H.; Ni Dhubhghaill, O. M.; Pubanz, D.; Helm, L.; Lebedev, Y. S.; Schlaepfer, W.; Merbach, A. E. *J. Am. Chem. Soc.* **1996**, *118*, 9333−9346.

(50) Cossy, C.; Helm, L.; Powell, D. H.; Merbach, A. E. *New J. Chem.* **1995**, *19*, 27−35.

binding to HSA (2-fold) but significantly reduced (17-fold) upon binding to RSA. Assuming a similar reduction in the water exchange rate for the gadolinium analogue, MS-325, the difference in water exchange would explain the observed differences in relaxivity when MS-325 was bound to the various serum albumins.

To confirm that water exchange is slower when **DyL1** is bound to RSA, variable-temperature r_2 measurements were made. Relaxation induced by the dysprosium complex is less efficient than that of the gadolinium complex, so at 310 K, **DyL1** is in fast exchange ($T_{2m} > \tau_m$). Relaxivity should increase with decreasing temperature because τ_R is getting longer (eq 5). However, at low enough temperature, the residency time becomes longer than T_2 of the bound water and now slow water exchange should limit r_2. Figure 4 shows that for **DyL1** bound to RSA relaxivity reaches a peak at ca. 290 K and then decreases whereas for **DyL1** bound to HSA the relaxivity maximum is not reached but is predicted to be about 265 K. The observation of crossover from fast exchange to slow exchange for the **DyL1**/RSA system and not for the **DyL1**/HSA system over this temperature range is conclusive evidence that water exchange is faster at **DyL1** bound to HSA.

Conclusion

The noncovalent association of a metal complex with a protein can alter water exchange at the metal ion. This has important consequences for the design of new MRI contrast agents that often rely on protein binding for targeting and improving relaxivity because slow water exchange can limit relaxivity. Exchanging Gd^{III} for another Ln^{III} is straightforward and the last step in the synthesis of the complex. Surrogate lanthanide complexes provide direct access to specific molecular parameters that are only sampled in aggregate when measuring the relaxivity of gadolinium complexes. Rotational correlation times can be readily obtained from 1D ^{1}H NMR spectra of Yb^{III} complexes; water exchange rates for protein-bound complexes are accessible through the effect of the Dy^{III} analogue on solvent relaxation rates; and Eu^{III} fluorescence decay provides insight into the hydration number. The techniques described in this paper are generally applicable to other Gd^{III} complexes being investigated for protein targeting and have sufficient sensitivity to be effective in the high micromolar to low millimolar concentration regime.

Acknowledgment is made to Qing Deng and Matt Greenfield for assistance with some of the HPLC analyses.

Supporting Information Available: Variable-temperature ^{1}H NMR, ^{1}H−^{1}H COSY NMR, and HPLC analysis of **YbL1**. This material is available free of charge via the Internet at http://pubs.acs.org.

IC070011U